Effects of Near-Surface Soil Moisture on GPS SNR Data: Development of a Retrieval Algorithm for Soil Moisture

Clara C. Chew, Eric E. Small, Kristine M. Larson, and Valery U. Zavorotny, *Fellow, IEEE*

***Abstract*—Global Positioning System (GPS) multipath signals can be used to infer volumetric soil moisture around a GPS antenna. While most GPS users concentrate on the signal that travels directly from the satellite to the antenna, the signal that is reflected by nearby surfaces contains information about the environment surrounding the antenna. The interference between the direct and reflected signals produces a modulation that can be observed in temporal variations of the signal-to-noise ratio (SNR) data recorded by the GPS receiver. Changes in the dielectric constant of the soil, which are associated with fluctuations in soil moisture, affect the effective reflector height, amplitude, and phase of the multipath modulation. Empirical studies have shown that these changes in SNR data are correlated with near-surface volumetric soil moisture. This study uses an electrodynamic single-scattering forward model to test the empirical relationships observed in field data. All three GPS interferogram metrics (effective reflector height, phase, and amplitude) are affected by soil moisture in the top 5 cm of the soil; surface soil moisture ($<$ 1-cm depth) exerts the strongest control. Soil type exerts a negligible impact on the relationships between GPS interferogram metrics and soil moisture. Phase is linearly correlated with surface soil moisture. The slope of the relationship is similar to that observed in field data. Amplitude and effective reflector height are also affected by soil moisture, although the relationship is nonlinear. Phase is the best metric derived from GPS data to use as a proxy for soil moisture variations.**

***Index Terms*—Global Positioning System (GPS), radar, reflectometry, remote sensing, soil.**

I. Introduction

NEAR-surface soil moisture has been the subject of numerous climate and land surface–atmosphere studies [1]–[3]. Soil moisture affects precipitation [4] via the partitioning of energy between the land and the atmosphere into sensible and latent heat fluxes [5].

Manuscript received December 1, 2011; revised May 13, 2012, August 27, 2012, and November 30, 2012; accepted December 22, 2012. This work was supported in part by the National Science Foundation (NSF) under Grants Atmospheric and Geospace Sciences (AGS) 0935725, Earth Sciences (EAR) 0948957, by EAR 1144221, and by the National Aeronautics and Space Administration under Grant NNH09ZDA001N.

C. C. Chew and E. E. Small are with the Department of Geological Sciences, University of Colorado, Boulder, CO 80309 USA (e-mail: clara.chew@colorado.edu; eric.tilton@colorado.edu).

K. M. Larson is with the Department of Aerospace Engineering, University of Colorado, Boulder, CO 80309 USA (e-mail: Kristine.larson@colorado.edu).

V. U. Zavorotny is with the Earth Systems Research Laboratory, National Oceanic and Atmospheric Administration, Boulder, CO 80305 USA (e-mail: valery.zavorotny@noaa.gov).

Digital Object Identifier 10.1109/TGRS.2013.2242332

Global Positioning System (GPS) Interferometric Reflectometry (GPS-IR) is a bistatic radar remote sensing technique that could improve knowledge of near-surface soil moisture as well as other environmental variables [6]–[8]. Signals transmitted from GPS satellites are in the L-band microwave region ($\sim$1.2 and 1.5 GHz) and penetrate further into the ground than signals of instruments using higher frequency bands [9]. Several studies have shown that GPS instruments can be used to infer soil moisture using information contained in the ground-reflected or multipath signal [10], [11]. However, the antennas in these studies have been altered in some way, either by making them more sensitive to multipath [12], [13] or by changing their orientation from the zenith-directed orientation used in GPS networks. These changes enhance the multipath signal. These studies also relied on receivers that were particularly designed for multipath measurements rather than commercial off-the-shelf instruments.

Recently, it has been shown that GPS instruments developed for tectonic studies and land surveying (here called geodetic-quality GPS instruments) are also highly sensitive to soil moisture in the top 5 cm of soil [14], [15]. A previous study by Zavorotny *et al.* [16] showed that an electrodynamic single-scattering forward model for typical soil moisture conditions produced qualitative changes in simulated GPS data that were consistent with the field observations. However, Zavorotny *et al.* [16] did not attempt to develop a retrieval algorithm to estimate soil moisture from GPS data. The aim of this study is to provide the theoretical basis for such an algorithm. This would allow GPS data collected with geodetic-quality instruments to be used to validate L-band soil moisture satellites such as Soil Moisture and Ocean Salinity (SMOS) [17] and Soil Moisture Active Passive (SMAP) [18]. We will first briefly review the characteristics of the observations and the model that will be used in this study, followed by an evaluation of different simulations.

II. GPS Data

A geodetic-quality GPS antenna receives energy from both the direct and ground-reflected signals (Fig. 1). Although dominated by the much stronger direct signal, the interference between the direct and reflected signals is also measurable. GPS receivers can be used to observe soil moisture variations because the dielectric constant of the ground is primarily a function of the soil moisture content [19]. This causes a change in the complex surface reflection coefficient and, hence, a change

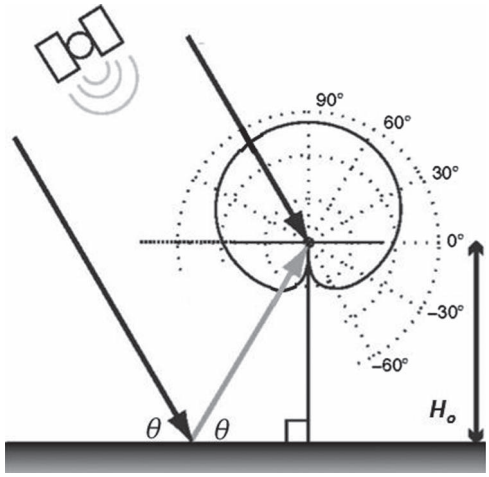

Fig. 1. (From [25]) Geometry of a multipath signal, for antenna height (H_o) and satellite elevation angle (θ). Bold black lines represent the direct signal transmitted from the satellite. The gray line is the reflected signal from the ground. The antenna's phase center is shown as the small dot. The solid line represents the gain pattern of the antenna. The radial distance between the antenna phase center and the solid line represents the strength of the antenna gain. Thus, an elevation angle of 90° has an antenna gain that is ∼40% stronger than that for an elevation angle of 0°.

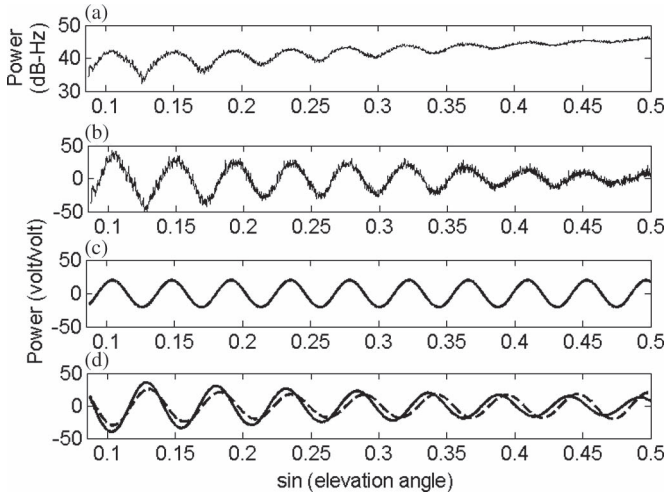

Fig. 2. (a) Observed SNR data from a geodetic-quality GPS receiver. (b) Same SNR interferogram from (a) that has had the direct component removed with a low-order polynomial and converted from decibel-hertz to a linear scale. (c) Best-fit approximation of the data from panel (b) using (1). (d) Two multipath modulations generated from the electrodynamic model. The dashed line represents a modulation resulting from wet soil; the solid line represents a modulation from a dry soil.

in the interference pattern observed in GPS data. Unlike airplane or satellite reflection experiments, ground GPS receivers observe a coherent interference pattern. The variations in the interference patterns result from a complex interaction between reflection coefficients and the antenna gain pattern, both of which vary with elevation angle. Given these complications, forward model simulations are the only practical way to guide development of a retrieval algorithm.

The effects of multipath in geodetic-quality GPS receivers can be observed in engineering data that measure the ratio of the signal power to the noise power spectral density or, simply, signal-to-noise ratio (SNR) data. A typical time series of SNR data from a GPS receiver is shown in Fig. 2(a). The slow change from 35 to 45 dB · Hz is due to the direct signal. The oscillations superimposed on the direct signal are caused by multipath signals reflected off the ground.

The geodetic community uses an entirely geometric description for observations of GPS multipath. With very few exceptions, the goal for these researchers has been to identify and remove the multipath effects [21]–[24]. For soil moisture sensing, the direct signal is not of interest and is typically removed with a low-order polynomial, leaving the SNR observations as shown in Fig. 2(b). We refer to SNR data where the direct signal effect has been removed as $\mathrm{SNR}_{\mathrm{mpi}}$, the subscript (multipath interference) indicating that variations are the result of interference between the reflected and direct signals. Geodesists use this expression to summarize how $\mathrm{SNR}_{\mathrm{mpi}}$ varies with elevation angle [Fig. 2(c)]

$$\mathrm{SNR}_{\mathrm{mpi}} = A_{\mathrm{mpi}} \cos\left(\frac{4\pi H_o}{\lambda}\sin\theta + \phi_{\mathrm{mpi}}\right) \tag{1}$$

where A_{mpi} scales with the intensity of ground reflections, θ is the satellite elevation angle (90° being defined as zenith), ϕ_{mpi} is phase, λ is the GPS signal wavelength, and H_o is the antenna height [14]. This expression shows no direct dependence on soil moisture or dielectric properties of the ground, although field observations indicate that both A_{mpi} and ϕ_{mpi} vary with soil moisture [14], [15]. The amplitude term includes the influence of both the gain pattern and multipath intensity. Although both antenna gain and multipath intensity vary with θ, the variation of A_{mpi} with θ is not large. Thus, as in previous analyses of $\mathrm{SNR}_{\mathrm{mpi}}$ data, we assume that A_{mpi} does not vary with θ [25]. Temporal fluctuations in A_{mpi} should depend only on the wetting of the soil, as the gain pattern itself does not change from day to day. Larson *et al.* showed that a correlation exists between A_{mpi} and rain events [25]. However, the observed effects of shallow soil moisture variations on ϕ_{mpi} are larger than those on A_{mpi}, as demonstrated by [14]. The forward model simulations of Zavorotny *et al.* [16] were consistent with these observations.

Larson *et al.* [15] explored an alternative approach for analyzing the changes in $\mathrm{SNR}_{\mathrm{mpi}}$ resulting from soil moisture fluctuations. The frequency of multipath modulations f_m present in $\mathrm{SNR}_{\mathrm{mpi}}$ data [e.g., Fig. 2(b)] varies with reflection characteristics [26]. f_m is related to the effective reflector height H_{eff}

$$H_{\mathrm{eff}} = \frac{1}{2} f_m \lambda. \tag{2}$$

Field observations show that H_{eff} varies with soil moisture fluctuations [15]. As with A_{mpi} and ϕ_{mpi}, the model results of Zavorotny *et al.* qualitatively supported these observations.

In the next section, we use the model of Zavorotny *et al.* [16] to develop a GPS soil moisture retrieval algorithm for a bare soil. For a given H_o, we quantify the variations in A_{mpi} and ϕ_{mpi} resulting from soil moisture fluctuations. We also quantify variations in H_{eff} that result from soil moisture fluctuations.

III. Methods

A. Forward Model and GPS Metric Definitions

1) Model Description and Development: The key points of the GPS simulator developed in [16] are that it fully represents the polarimetric characteristics of both the direct and reflected

GPS signals as they would be measured by geodetic-quality GPS antennas and receivers. The transmitted power from the GPS satellites to the Earth is primarily right-handed circularly polarized, as defined in [27], although upon reflection, part of the signal is converted to left-handed. The simulator then computes how much power would be received via the direct and the reflected signal path. Both left-handed and right-handed signals are fully defined in this simulator. To do so, the simulator uses a gain pattern for a geodetic-quality antenna measured in an anechoic chamber. The reflected signal is determined by the reflection characteristics (polarization and reflection coefficients) calculated over a 20-cm soil column stratified into 1-mm-thick layers. The simulator was not developed specifically for soil moisture applications, i.e., it could be used to investigate reflections from any stratified medium.

To calculate the reflection coefficients of the soil, volumetric soil moisture values were first converted to dielectric constants using relationships given in [19]. These relationships were derived from a semiempirical dielectric mixing model based on experimental observations and knowledge of how soil water should respond to an induced electric field [19]. The resulting dielectric constants were then converted to reflection coefficients using the small-perturbation method for a layered medium with permittivity variations [28]. Reflection coefficients were combined with a specified antenna radiation pattern to produce the $\mathrm{SNR}_{\mathrm{mpi}}$ interferograms. Examples of $\mathrm{SNR}_{\mathrm{mpi}}$ curves produced by the model for a dry and wet soil moisture profile are shown in Fig. 2(d).

2) Model Parameters: In this paper, we have restricted the analysis for satellite elevation angles between 5° and 30° (data below elevation angles of 5° are often obstructed by buildings and trees). These are the elevation angles most impacted by multipath—which is why they have been used in previous studies [14], [15]. The antenna was set to be 2.4 m above the ground, similar to many field installations. We varied the antenna height from 1 to 3 m to quantify the sensitivity of $\mathrm{SNR}_{\mathrm{mpi}}$ to this parameter. The GPS signal was set to have a wavelength of ∼24.4 cm, the wavelength for L2 civil signals used in previous GPS-IR applications [14], [15].

Environmental parameters were purposefully simplified so that the effect of soil moisture on $\mathrm{SNR}_{\mathrm{mpi}}$ data could be examined without complications from other factors, i.e., data were simulated for an area with no topography, surface roughness, or vegetation. Although we tested five soil textures, we will focus on results for a soil with a loamy texture.

3) Calculation of GPS $\mathrm{SNR}_{\mathrm{mpi}}$ Metrics: Three GPS metrics are discussed in this paper. Least squares estimation was used to determine ϕ_{mpi} and A_{mpi} from the simulated $\mathrm{SNR}_{\mathrm{mpi}}$ data, for the specified H_o. Note that, by setting H_o, the frequency of the $\mathrm{SNR}_{\mathrm{mpi}}$ interferogram is constant. The values of ϕ_{mpi} were zeroed with respect to the minimum phase value simulated, i.e., phase values that ranged from 200° to 230° are reported here as 0°–30°.

Separately, an effective reflector height (H_{eff}) was calculated from the simulated $\mathrm{SNR}_{\mathrm{mpi}}$ data using a Lomb–Scargle periodogram [20], a method of least squares spectral analysis that calculates the spectral power for a range of frequencies. The frequency with the greatest power is then converted to H_{eff} using (2). In all the simulations discussed as follows, H_{eff} is within several centimeters of H_o. An oversampling parameter was used in the Lomb–Scargle periodogram that allowed this metric to be estimated with a precision of 0.3 cm. For simplicity, we will refer to ϕ_{mpi}, A_{mpi}, and H_{eff} as GPS interferogram metrics.

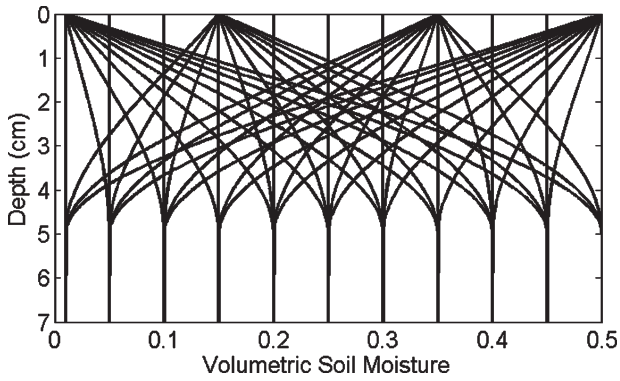

Fig. 3. Simulated soil moisture profiles. Only the top 7 cm of the profiles is shown, as soil moisture values were constant below 5-cm depth.

B. Soil Moisture Profiles

1) Constant Profiles and Simple Wetting and Drying Profiles: We first calculated GPS interferogram metrics for soil profiles with uniform soil moisture throughout a 20-cm modeled domain. The soil moisture profiles were discretized to have soil layers that were 1 mm thick. We report our results as volumetric soil moisture, meaning the fraction of the total volume of a soil layer filled with water (0–1.0). For the uniform soil profile simulations, we varied volumetric soil moisture values from 0.01 to 0.50. Although it is unlikely that the loam soil modeled in this study would have a residual water content of 0.01, we extended our analysis to this value to test the full range of possible relationships between GPS metrics and soil moisture.

We also constructed simple soil moisture profiles with the same 20-cm domain and 1-mm vertical discretization for cases when the surface soil is wetter and dryer than the soil as follows (Fig. 3). In these profiles, soil moisture was constant below 5 cm. The model was also run with soil profiles that had moisture variations with depth down to 10 cm, but no significant differences were found compared with results from the aforementioned profiles. It was thus deemed reasonable to keep soil moisture values constant below 5-cm depth. For profiles that vary with depth, the surface volumetric soil moisture value is denoted as SM_0, and the average volumetric soil moisture value for the top 5 cm of soil is denoted as SM_{0-5}.

2) Field Data: We used soil moisture data from an unirrigated agricultural wheat field to provide a representation of a set of realistic soil moisture profiles. The data used to generate these profiles were collected using 11 Campbell Scientific 616 water content reflectometers: Five were buried at a depth of 2.5 cm, five were buried at a depth of 7.5 cm, and one was buried at a depth of 20 cm. Over 230 consecutive days of data were used to provide soil moisture profiles for the model.

We used the reflectometer data as point measurements of soil moisture at the installation depth. However, the geometry of

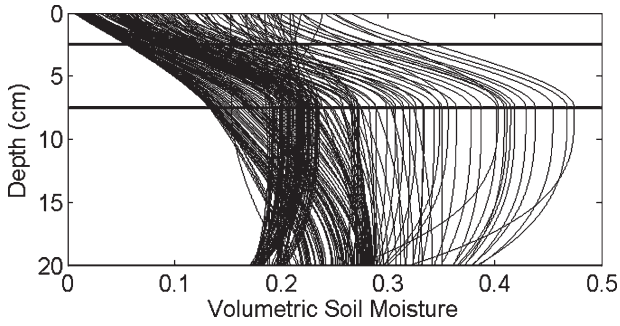

Fig. 4. Interpolated soil moisture profiles, given three point measurements at (horizontal lines) 2.5, 7.5, and 20 cm.

CS616 probes actually yields a measurement that integrates soil moisture over a depth of approximately 5 cm [29]. We also used the factory calibration for the soil moisture probes, even though a calibration developed specifically for the soil at the site should yield more accurate volumetric soil moisture values. Neither of these issues is a source of error in our study because we did not attempt to compare simulated SNR data to actual SNR data collected from this field. These data were only used to provide guidance on the type and extent of soil moisture profiles that could potentially exist in field settings. We constructed profiles from these point measurements using a piecewise cubic Hermite method to interpolate data between the measurement depths (Fig. 4). The interpolation of these measurements does not exactly match the profiles that exist in the field but was useful in determining common soil moisture gradients that exist within the soil column. More sophisticated physically based modeling or other retrieval algorithms could be used to simulate near-surface soil moisture as in [30], but this was beyond the scope of this study. Only the relationship between soil moisture and ϕ_{mpi} will be shown for these profiles; relationships were similar for the other metrics.

IV. Results

A. Relationships Between GPS Metrics and Soil Moisture Profiles

1) Phase: Given uniform soil moisture profiles, ϕ_{mpi} exhibits a positive and nearly linear relationship with volumetric soil moisture (Fig. 5). Phase varies by 30° over the range of dry to wet uniform soil moisture profiles that we tested. The slope of this relationship or the sensitivity of ϕ_{mpi} to uniform soil moisture is $65.1^\circ \cdot \mathrm{cm}^3 \cdot \mathrm{cm}^{-3}$. This means that a 20° change in ϕ_{mpi} would correspond to a 0.31 change in volumetric soil moisture. This relationship is the same regardless of soil type and does not depend on the height of the antenna H_o (Table I).

For soil moisture profiles that vary with depth, ϕ_{mpi} does not vary consistently with SM_{0-5}. Fig. 5 shows the relationship between SM_{0-5} and ϕ_{mpi} for a variety of different soil moisture profiles, a subset of which is depicted in the inset. The subsets of profiles, labeled a–k in the figure, all have the same surface volumetric soil moisture (0.15). However, the volumetric soil moisture beneath the surface may be lower (profiles a–c) or higher (e–k) than that at the surface. As a result, these profiles have different values of SM_{0-5}. As can be seen in the figure,

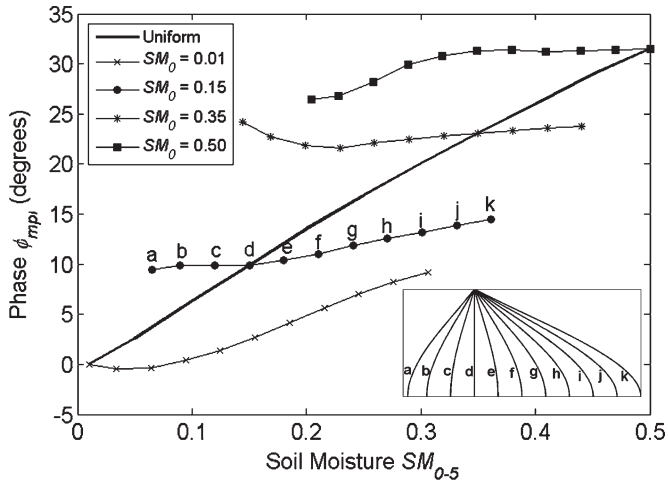

Fig. 5. Relationship between phase ϕ_{mpi} and volumetric soil moisture averaged over the top 5 cm SM_{0-5}. The unmarked line indicates results for profiles in which soil moisture did not vary with depth. For these cases, the surface soil moisture is equal to SM_{0-5}. Other data are grouped by the value of soil moisture at the surface SM_0 (lines with symbols). Within each group, each point corresponds to one profile in Fig. 3. The inset provides an example of one group of profiles with the same surface soil moisture (0.15), taken from Fig. 3.

TABLE I
Slopes and r_2 Values for Linear Regressions of Soil Moisture and Phase Using Different Soil Types for $H_o = 2.4$ m. Values for Loam Soil With $H_o = 1.0$ m and $H_o = 3.0$ m Are Also Shown. Linear Regressions Are for Uniform Soil Moisture Profiles. Results Indicate That the Relationship Between Soil Moisture and Phase Is Similar Regardless of Soil Type

Soil Type	Slope (deg cm^3 cm^{-3})	r^2 value
Sandy Loam	65.8	0.996
Loam	65.1	0.997
Loam (H_o = 1m)	66.9	0.998
Loam (H_o = 3m)	65.7	0.997
Silt Loam I	65.0	0.997
Silt Loam II	66.1	0.998
Silty Clay	65.3	0.998

the relationship between SM_{0-5} and ϕ_{mpi} for these profiles is not linear, and the slope is much smaller than that for uniform moisture profiles. This is true for the other groups of profiles that have moisture variations over depth. ϕ_{mpi} for these profiles appears to depend predominantly on the surface soil moisture value and not strongly on SM_{0-5}.

2) Amplitude: For uniform soil moisture profiles, soil moisture and A_{mpi} have a linear inverse relationship (Fig. 6). This relationship does not hold when the soil moisture is below 0.10. For these dry values, A_{mpi} does not respond significantly to soil moisture changes.

For moisture profiles that vary with depth, SM_{0-5} and A_{mpi} are either positively related or unrelated, depending on the value of the surface soil moisture. This is in contrast to the linear inverse relationship that exists between uniform moisture profiles and amplitude. For the nonuniform moisture profiles that have relatively wet SM_0 values (asterisks or squares in Fig. 6), A_{mpi} does not vary with SM_{0-5}. For the profiles with lower SM_0 (circles or "x"s in Fig. 6), A_{mpi} is positively related to SM_{0-5}. As is the case for ϕ_{mpi}, it appears that amplitude also depends primarily on surface soil moisture, not on SM_{0-5}.

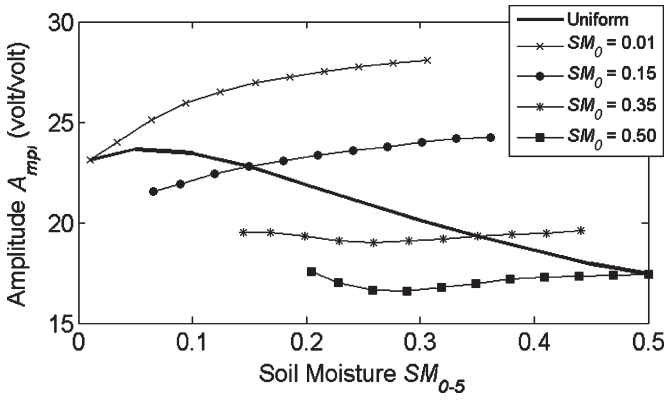

Fig. 6. Relationship between amplitude A_{mpi} and soil moisture averaged over the top 5 cm SM_{0-5}. The unmarked line indicates results for profiles in which soil moisture did not vary with depth. Other data are grouped by the value of soil moisture at the surface, as in Fig. 5 (lines with symbols).

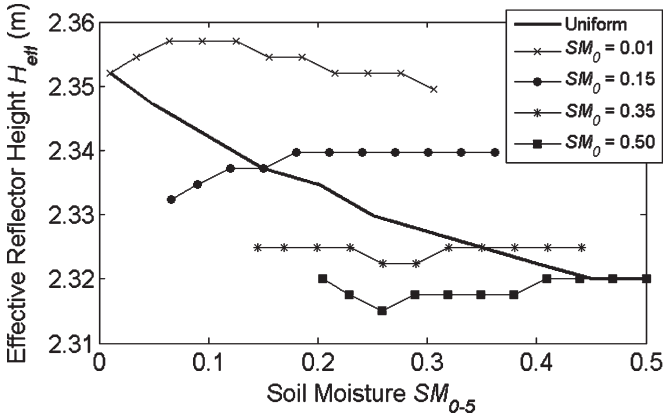

Fig. 7. Relationship between effective reflector height H_{eff} and volumetric soil moisture averaged over the top 5 cm SM_{0-5}. The unmarked line indicates results for profiles in which soil moisture did not vary with depth. Other data are grouped by the value of soil moisture at the surface, as in Fig. 5 (lines with symbols).

3) Effective Reflector Height: For uniform moisture profiles, as the soil becomes wetter, the height estimated from the Lomb–Scargle periodogram (H_{eff}) decreases (Fig. 7). The variation in H_{eff} is approximately 3.3 cm for the range of soil moisture values tested.

As with both ϕ_{mpi} and A_{mpi}, once soil moisture profiles are allowed to vary with depth, the dependence of H_{eff} on SM_{0-5} is neither strong nor consistent. As is seen in Fig. 7, H_{eff} varies by < 1 cm with SM_{0-5} for moisture profiles that vary with depth. Thus, H_{eff} appears to be primarily influenced by SM_0. The millimeter differences in H_{eff} that result from moisture variations at depth would be difficult to distinguish in field measurements. However, the centimeter-level changes between uniform wet and dry profiles should be observable, as previously shown by [14] and [15].

B. Field Profiles and Phase

In this section, we present results from $\mathrm{SNR}_{\mathrm{mpi}}$ data that were simulated using soil moisture profiles interpolated from field data (see Fig. 4 for interpolated moisture profiles). SM_0 and ϕ_{mpi} have a near-perfect correlation with an r_2 value of 0.997 (Fig. 8) despite the wide range of soil moisture profiles

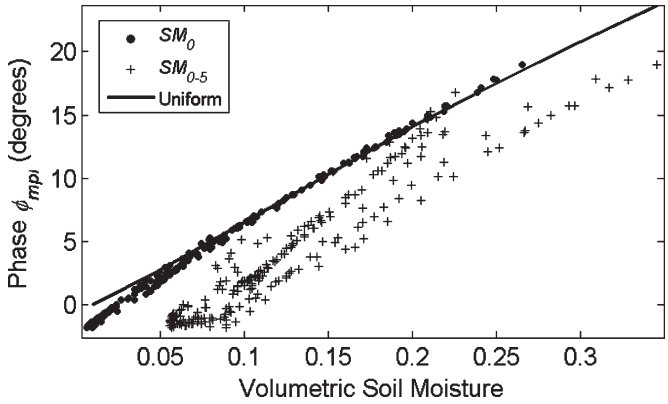

Fig. 8. Relationship between phase ϕ_{mpi} and volumetric soil moisture interpolated from field data. Solid dots correspond to surface soil moisture SM_0 extrapolated from field measurements at 2.5- and 7.5-cm depths. The plus (+) signs correspond to soil moisture, averaged over the top 5 cm of the interpolated field profiles SM_{0-5}. The solid line is the relationship between phase and soil moisture for profiles that do not vary with depth, as in Fig. 5.

tested. This indicates that ϕ_{mpi} is highly dependent on changes in surface soil moisture. The correlation between ϕ_{mpi} and SM_{0-5} is still excellent $(r^2 = 0.91)$ (Fig. 8). However, some of this correlation is the result of the covariance between SM_{0-5} and SM_0 rather than the effects of soil moisture at depth on $\mathrm{SNR}_{\mathrm{mpi}}$. Soil moisture at 0 cm was extrapolated from the value measured at 2.5 cm using the gradient measured at depths of 2.5 and 7.5 cm. Thus, the predicted SM_0 was always tightly coupled with this gradient. The covariance between SM_0 and the soil moisture at deeper depths may not be as strong in the field. Nearly all of the interpolated profiles have dryer soil at the surface than at depth. Therefore, each $\phi_{\mathrm{mpi}} - \mathrm{SM}_{0-5}$ point plots to the right of the corresponding $\phi_{\mathrm{mpi}} - \mathrm{SM}_0$ point. This is consistent with the results shown in Fig. 5 (e.g., points e–k), for cases when the soil is drier at the surface than at depth.

A_{mpi} and H_{eff} have similar correlations with the soil moisture profiles that were interpolated from field measurements. The r^2 value for the correlation between A_{mpi} and SM_0 is 0.81, and its value is 0.63 for the correlation between A_{mpi} and SM_{0-5}. The smaller r^2 (compared to that for ϕ_{mpi} and soil moisture) is expected, given the complex relationship between A_{mpi} and soil moisture (Fig. 6). The r^2 value for the correlation between H_{eff} and SM_0 is 0.97; between H_{eff} and SM_{0-5}, it is 0.86.

V. Discussion

Field observations indicate that ϕ_{mpi} and soil moisture have a linear relationship with a slope of $65.1^\circ \cdot \mathrm{cm}^3 \cdot \mathrm{cm}^{-3}$. The simulated results presented in this paper agree with empirical findings (Fig. 9). However, the slope of the relationship between ϕ_{mpi} and soil moisture is $\sim$20% greater in the field observations than that produced by the model. There are two possible reasons for this discrepancy. First, the *in situ* probes provided an estimate of SM_{0-5}, whereas the ϕ_{mpi} measured in the field is more directly related to SM_0 [15]. Second, the field observations were not from sites completely devoid of vegetation, and vegetation may change the sensitivity of ϕ_{mpi} to soil moisture.

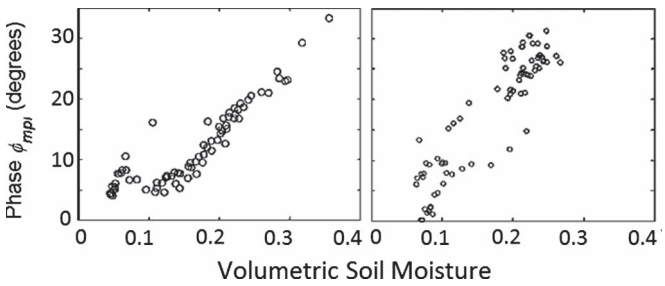

Fig. 9. (Left) Results from [15] that show the empirical relationship between phase and volumetric soil moisture from a field site in Marshall, CO. (Right) Results from a field site in Oklahoma that show a similar relationship between phase and volumetric soil moisture. In both cases, the field measurements of soil moisture represent an approximate average over the top 5 cm of the soil profiles [15].

It is well known that L-band signals penetrate further into soils that are dry than soils that are wet [31]. It is possible to calculate the effective penetration depth, which is usually defined as the depth at which the signal's power has been attenuated to $1/e$ of its value at the soil surface [31]. For passive L-band remote sensing, this depth varies from 0.1 to 1 m, depending on whether the soil is wet or dry [31].

This definition of penetration depth, however, is not appropriate for defining the depth of soil that significantly affects $\mathrm{SNR}_{\mathrm{mpi}}$. The signal may penetrate to this depth in the soil. However, this does not mean that a significant portion of the signal returns back through the soil surface to the antenna. In addition, $\mathrm{SNR}_{\mathrm{mpi}}$ depends not only upon the depth at which the wave was reflected but also on the dielectric properties of the soil. Other studies have also addressed this issue [31], [32]. The term for the region of soil that affects the overall signal is sometimes referred to as the "moisture sensing depth" and is often taken to be one-tenth of a wavelength in the soil, which corresponds to less than 2 cm for L-band [31].

Fig. 8 indicates that the surface soil moisture value is the determining factor in ϕ_{mpi}. This is to be expected, since low elevation angles have higher surface reflection coefficients than higher angles [28]. It appears that the observed correlations between ϕ_{mpi} and soil moisture averaged over the top 5 cm of soil, like those shown in Fig. 8, result from a combination of the following: 1) strong covariance between SM_0 and soil moisture at 2.5 cm and 2) soil moisture at deeper depths affecting the overall signal. Although the relative contributions of these two factors were not quantitatively compared, our results show that the correlation between SM_0 and soil moisture at 2.5 cm is the driving factor in the correlation between the GPS interferogram metrics A_{mpi}, H_{eff}, and ϕ_{mpi} and SM_{0-5}. It is possible that other aspects of the SNR interferogram besides A_{mpi}, H_{eff}, and ϕ_{mpi} are affected by soil moisture at depth. The investigation into what those aspects might be, however, was outside the scope of this study.

VI. Conclusion

The physical model used in this study indicates that phase (ϕ_{mpi}), amplitude (A_{mpi}), and effective reflector height (H_{eff}) derived from simulated $\mathrm{SNR}_{\mathrm{mpi}}$ data are sensitive to changes in soil moisture. ϕ_{mpi} is linearly correlated with volumetric soil moisture, which is consistent with previously published field observations. The slope from the simulated data is similar to that observed at two field sites. A_{mpi} and H_{eff} also vary with soil moisture, although these relationships are not as straightforward as that for ϕ_{mpi}. Thus, ϕ_{mpi} is the best estimator of soil moisture change for bare soil conditions. All three GPS interferogram metrics are most sensitive to changes in surface soil moisture, compared to soil moisture averaged over the top 5 cm of the soil column. The slope estimated from these simulations can be used in a retrieval algorithm to convert ϕ_{mpi} observations into volumetric soil moisture. A comprehensive retrieval should also include the effects of surface roughness, vegetation, and soil temperature. These variables should be included in future modeling efforts in order to determine their effect on GPS interferogram metrics.

Acknowledgment

The authors would like to thank the University Navstar Consortium (UNAVCO) for their continued assistance.

References

[1] E. Njoku, V. Lakshmi, and P. O'Neill, "Soil moisture field experiment special issue," *Remote Sens. Environ.*, vol. 92, no. 4, pp. 425–426, Sep. 2004.

[2] P. Rosnay, J. C. Calvet, Y. Kerr, J. P. Wigneron, F. Lemaître, M. Escorihuela, J. Sabater, K. Saleh, J. Barrié, G. Bouhours, L. Coret, G. Cherel, G. Dedieu, R. Durbe, N. Fritz, F. Froissar, J. Hoedjes, A. Kruszewski, F. Lavenu, D. Suquia, and P. Waldteufel, "SMOSREX: A long term field campaign experiment for soil moisture and land surface processes remote sensing," *Remote Sens. Environ.*, vol. 102, no. 3/4, pp. 377–389, Jun. 2006.

[3] J. M. Sabater, C. Rüdiger, J. C. Calvet, N. Fritz, L. Jarlan, and Y. Kerr, "Joint assimilation of surface soil moisture and LAI observations into a land surface model," *Agr. Forest Meteorol.*, vol. 148, no. 8/9, pp. 1362–1373, Jul. 2008.

[4] A. Betts, J. Ball, A. Beljaars, M. Miller, and P. Viterbo, "The land surface–atmosphere interaction: A review based on observational and global modeling perspectives," *J. Geophys. Res.*, vol. 101, no. D3, pp. 7209–7225, Jan. 1996.

[5] A. Robock, K. Vinnikov, G. Srinivasan, J. Entin, S. Hollinger, N. Speranskaya, S. Liu, and A. Namkhai, "The global soil moisture data bank," *Bull. Amer. Meteorol. Soc.*, vol. 81, no. 6, pp. 1281–1299, Jun. 2000.

[6] S. Jin and A. Komjathy, "GNSS reflectometry and remote sensing: New objectives and results," *Adv. Space Res.*, vol. 46, no. 2, pp. 111–117, Jul. 2010.

[7] S. Jin, G. Feng, and S. Gleason, "Remote sensing using GNSS signals: Current status and future directions," *Adv. Space Res.*, vol. 47, no. 10, pp. 1645–1653, May 2011.

[8] Q. Li, S. Reboul, J. B. Choquel, M. Benjelloun, and A. Gardel, "Beach soil moisture measurement with a land reflected GPS bistatic radar technique," in *Proc. New Trends Environ. Monit. Passive Syst.*, 2008, pp. 1–6.

[9] M. Nolan and D. Fatland, "Penetration depth as a DInSAR observable and proxy for soil moisture," *IEEE Trans. Geosci. Remote Sens.*, vol. 41, no. 3, pp. 532–537, Mar. 2003.

[10] N. Rodriguez-Alvarez, X. Bosch-Lluis, A. Camps, M. Vall-Ilossera, E. Valencia, J. F. Marchan-Hernandez, and I. Ramos-Perez, "Soil moisture retrieval using GNSS-R techniques: Experimental results over a bare soil field," *IEEE Trans. Geosci. Remote Sens.*, vol. 47, no. 11, pp. 3616–3624, Nov. 2009.

[11] N. Rodriguez-Alvarez, A. Camps, M. Vall-Ilossera, X. Bosch-Lluis, A. Monerris, I. Ramos-Perez, E. Valencia, J. F. Marchan-Hernandez, J. Martinez-Fernandez, G. Baroncini-Turricchia, C. Pérez-Gutiérrez, and N. Sánchez, "Land geophysical parameters retrieval using the interference pattern GNSS-R technique," *IEEE Trans. Geosci. Remote Sens.*, vol. 49, no. 1, pp. 71–84, Jan. 2011.

[12] N. Pierdicca, L. Guerriero, R. Giusto, M. Brogioni, A. Egido, and N. Floury, "GNSS reflections from bare and vegetated soils: Experimental validation of an end-to-end simulator," in *Proc. IEEE IGARSS*, Vancouver, Canada, 2011, pp. 4371–4374.

[13] R. Kato, H. Saito, and S. Fukuda, "Experimental study for GNSS-R polarimetry," in *Proc. IEEE IGARSS*, Vancouver, Canada, 2011, pp. 2853–2856.
[14] K. Larson, E. Small, E. Gutmann, A. Bilich, J. Braun, and V. Zavorotny, "Use of GPS receivers as a soil moisture network for water cycle studies," *Geophys. Res. Lett.*, vol. 35, no. 24, p. L24405, Dec. 2008.
[15] K. Larson, J. Braun, E. Small, V. Zavorotny, E. Gutmann, and A. Bilich, "GPS multipath and its relation to near-surface soil moisture content," *IEEE J. Sel. Topics Appl. Earth Observ. Remote Sens.*, vol. 3, no. 1, pp. 91–99, Mar. 2010.
[16] V. Zavorotny, K. Larson, J. Braun, E. Small, E. Gutmann, and A. Bilich, "A physical model for GPS multipath caused by land reflections: Toward bare soil moisture retrievals," *IEEE J. Sel. Topics Appl. Earth Observ. Remote Sens.*, vol. 3, no. 1, pp. 100–110, Mar. 2010.
[17] M. Berger, A. Camps, J. Font, Y. Kerr, J. Miller, J. Johannessen, J. Boutin, M. R. Drinkwater, N. Skou, N. Floury, M. Rast, H. Rebhan, and E. Attema, "Measuring ocean salinity with ESA's SMOS mission," *ESA Bull.*, vol. 111, no. 113f, pp. 113–121, Aug. 2002.
[18] D. Entekhabi, E. Njoku, P. O'Neill, K. Kellogg, W. Crow, W. Edelstein, J. Entin, S. Goodman, T. Jackson, J. Johnson, J. Kimball, J. Piepmeier, R. Koster, N. Martin, K. McDonald, M. Moghaddam, S. Moran, R. Reichle, J. Shi, M. Spencer, S. Thurman, T. Leung, and J. Van Zyl, "The Soil Moisture Active Passive (SMAP) mission," *Proc. IEEE*, vol. 98, no. 5, pp. 704–716, May 2010.
[19] M. Hallikainen, F. Ulaby, M. Dobson, M. El-Rayes, and L. Wu, "Microwave dielectric behavior of wet soil—Part I: Empirical models and experimental observations," *IEEE Trans. Geosci. Remote Sens.*, vol. GE-23, no. 1, pp. 25–34, Jan. 1985.
[20] W. H. Press, S. A. Teukolsky, W. T. Vetterling, and B. P. Flannery, *Numerical Recipes in Fortran 77*, 2nd ed, vol. 1. New York, USA: Cambridge Univ. Press, 1992, pp. 569–573.
[21] A. Bilich, K. M. Larson, and P. Axelrad, "Modeling GPS phase multipath with SNR: Case study from the Salar de Uyuni, Boliva," *J. Geophys. Res.*, vol. 113, no. B4, p. B04401, Apr. 2008.
[22] J. K. Ray and M. E. Cannon, "Synergy between global positioning system code, carrier, signal-to-noise ratio multipath errors," *J. Guid., Control, Dyn.*, vol. 24, no. 1, pp. 54–63, Jan. 2001.
[23] A. Reichert and P. Axelrad, "GPS carrier phase multipath reduction using SNR measurements to characterize an effective reflector," in *Proc. ION GPS*, 1999, pp. 1951–1960.
[24] C. Comp and P. Axelrad, "Adaptive SNR-based carrier phase multipath mitigation technique," *IEEE Trans. Aerosp. Electron. Syst.*, vol. 34, no. 1, pp. 264–276, Jan. 1998.
[25] K. M. Larson, E. E. Small, E. Gutmann, A. Bilich, P. Axelrad, and J. Braun, "Using GPS multipath to measure soil moisture fluctuations: Initial results," *GPS Solutions*, vol. 12, no. 3, pp. 173–177, Jul. 2008.
[26] P. Axelrad, K. Larson, and B. Jones, "Use of the correct satellite repeat period to characterize and reduce site specific multipath errors," in *Proc. ION GNSS 18th Int. Tech. Meeting Satellite Div.*, 2005, pp. 2638–2648.
[27] Global Positioning System Directorate. (2011). *Navstar GPS Space Segment/User Segment L1C Interface*, El Segundo, CA, USA, IS-GPS-800B. [Online]. Available: http://www.gps.gov/technical/icwg/
[28] I. M. Fuks and A. G. Voronovich, "Wave diffraction by rough interfaces in an arbitrary plane-layered medium," *Waves Random Media*, vol. 10, no. 2, pp. 253–272, Apr. 2000.
[29] F. Ferre, J. Knight, D. Rudolph, and R. Kachanoski, "The sample areas of conventional and alternative time domain reflectometry probes," *Water Resources Res.*, vol. 34, no. 11, pp. 2971–2979, Jan. 1998.
[30] J. P. Walker, G. R. Willgoose, and J. D. Kalma, "One-dimensional soil moisture profile retrieval by assimilation of near-surface observations: A comparison of retrieval algorithms," *Adv. Water Resources*, vol. 24, no. 6, pp. 631–650, Jun. 2001.
[31] E. Njoku and D. Entekhabi, "Passive microwave remote sensing of soil moisture," *J. Hydrol.*, vol. 184, no. 1/2, pp. 101–129, Oct. 1996.
[32] F. Ulaby, P. Dubois, and J. Van Zyl, "Radar mapping of surface soil moisture," *J. Hydrol.*, vol. 184, no. 1/2, pp. 57–84, Oct. 1996.

Clara C. Chew received the B.A. degree in environmental studies from Dartmouth College, Hanover, NH, USA, in 2009. She is currently working toward the Ph.D. degree in geological sciences in the Department of Geological Sciences, University of Colorado, Boulder, CO, USA.

Her research interests include surface hydrology and remote sensing.

Eric E. Small received the B.A. degree in geological sciences from Williams College, Williamstown, MA, USA, in 1993 and the Ph.D. degree in earth sciences from the University of California, Santa Cruz, CA, USA, in 1998.

He is a Professor with the Department of Geological Sciences, University of Colorado, Boulder, CO, USA. His research is focused on land surface hydrology.

Kristine M. Larson received the B.A. degree in engineering sciences from Harvard University, Cambridge, MA, USA, in 1985, and the Ph.D. degree in geophysics from the Scripps Institution of Oceanography, University of California at San Diego, La Jolla, CA, USA, in 1990.

From 1988 to 1990, she was a member of the technical staff at Jet Propulsion Laboratories, California Institute of Technology, Pasadena. Since 1990, she has been a Professor with the Department of Aerospace Engineering Sciences, University of Colorado, Boulder, CO, USA. Her research interests are focused on developing new applications and techniques for GPS.

Valery U. Zavorotny (M'01–SM'03–F'10) received the M.Sc. degree in radio physics from Gorky State University, Gorky, Russia, in 1971 and the Ph.D. degree in physics and mathematics from the Institute of Atmospheric Physics, Union of Soviet Socialist Republics Academy of Sciences, Moscow, Russia, in 1979.

From 1971 to 1990, he was a Research Scientist with the Institute of Atmospheric Physics, USSR Academy of Sciences. In 1990, he joined Lebedev Physical Institute, Moscow. In 1991–2000, he was a Cooperative Institute for Research in Environmental Sciences Research Associate with the Environmental Technology Laboratory (currently called Earth Systems Research Laboratory together with five other laboratories), National Oceanic and Atmospheric Administration, Boulder, CO, USA, where he became a Physicist in 2000. His research interests include theory of wave propagation through random media, wave scattering from rough surfaces, and ocean and land remote sensing applications.

Dr. Zavorotny is a member of International Union of Radio Science (Commission F) and the American Geophysical Union.